



Universiteit
Leiden
The Netherlands

Configuration of Spheroidene in the Photosynthetic Reaction Center of *Rhodobacter sphaeroides*: A Comparison of Wild-Type and Reconstituted R26

Mathies, G.; Hemert, M.C. van; Gast, P.; Sai Sankar Gupta, K.B.; Frank, H.A.; Lugtenburg, J.; Groenen, E.J.J.

Citation

Mathies, G., Hemert, M. C. van, Gast, P., Sai Sankar Gupta, K. B., Frank, H. A., Lugtenburg, J., & Groenen, E. J. J. (2011). Configuration of Spheroidene in the Photosynthetic Reaction Center of *Rhodobacter sphaeroides*: A Comparison of Wild-Type and Reconstituted R26. *The Journal Of Physical Chemistry A*, 115(34), 9552-9556. doi:10.1021/jp112413d

Version: Publisher's Version

License: [Licensed under Article 25fa Copyright Act/Law \(Amendment Taverne\)](#)

Downloaded from: <https://hdl.handle.net/1887/3570972>

Note: To cite this publication please use the final published version (if applicable).

Configuration of Spheroidene in the Photosynthetic Reaction Center of *Rhodobacter sphaeroides*: A Comparison of Wild-Type and Reconstituted R26

Guinevere Mathies,^{*,†} Marc C. van Hemert,[‡] Peter Gast,[†] Karthick B. Sai Sankar Gupta,[‡] Harry A. Frank,[§] Johan Lugtenburg,[‡] and Edgar J. J. Groenen^{*,†}

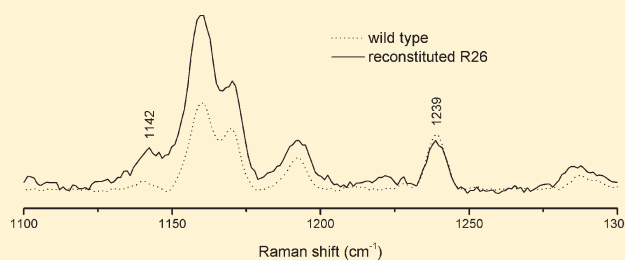
[†]Department of Molecular Physics, Huygens Laboratory, Leiden University, The Netherlands

[‡]Department of Chemistry, Gorlaeus Laboratories, Leiden University, The Netherlands

[§]Department of Chemistry, University of Connecticut, Storrs, Connecticut, United States

S Supporting Information

ABSTRACT: We compare the resonance Raman spectra acquired at two excitation wavelengths, 496.5 and 514.5 nm, of spheroidene in the wild-type reaction center of *Rhodobacter sphaeroides* and reconstituted into the reaction center of the *Rhodobacter sphaeroides* mutant R26. Our earlier work showed that the reconstituted R26 reaction center holds spheroidene in two configurations: 15,15'-*cis* and another configuration. Here we show that in the wild-type reaction center only 15,15'-*cis* spheroidene is present. In the resonance Raman spectra of the reconstituted R26 reaction centers, a transition is identified that arises exclusively from the second configuration. According to density-functional-theory calculations, this transition is specific for the 13,14-*cis* configuration.



INTRODUCTION

The primary process of bacterial photosynthesis is a trans-membrane charge separation. The minimum structural unit capable of producing the charge separation is an integral membrane complex termed the reaction center (RC), which was first isolated from the purple photosynthetic bacterium *Rhodobacter (Rb.) sphaeroides*.¹ Like all bacterial RCs, the RC of *Rb. sphaeroides* contains a carotenoid. If excess light is supplied to the RC, a triplet state of the primary donor is generated, which can result in the formation of singlet oxygen. The carotenoid quenches this triplet state through energy transfer, which produces a triplet carotenoid.^{2–4} To understand this photoprotective mechanism, it is important to know the structure of the carotenoid in the RC.

The carotenoid present in anaerobically grown *Rb. sphaeroides* RCs is spheroidene (see Figure 1). Early spectroscopic studies suggested that spheroidene assumes a *cis* configuration in the RC.^{5,6} Comparison of the resonance Raman spectra of spheroidene in RCs with resonance Raman spectra of *cis* isomers of β -carotene shows a strong resemblance between spheroidene in the RC and 15,15'-*cis* β -carotene.^{7,8} Both spectra display a clear band around 1240 cm^{-1} , which is not observed in the resonance Raman spectra of other *cis* isomers of β -carotene.

The structures of the RCs from three wild-type strains are known from X-ray diffraction.^{9–11} The presence of spheroidene in a 15,15'-*cis* configuration is consistent with the electron density map, but the resolution of these structures is insufficient to position a *cis* bond uniquely. In 2000, the electron density map

of the RC from the mutant AM260W of *Rb. sphaeroides*, which contains spheroidenone, was determined by X-ray diffraction and clearly favored a 15,15'-*cis* configuration above a 13,14-*cis* configuration.^{12,13}

In a long-term project, we have contributed to the study of the configuration of spheroidene in the RC of *Rb. sphaeroides* by combining resonance Raman spectroscopy with density-functional-theory (DFT) calculations.^{14–17} RCs from the carotenoidless mutant *Rb. sphaeroides* R26 were reconstituted with isotopically labeled spheroidenes. The use of specific ¹³C- and ²H-labeled spheroidenes enabled the assignment of normal modes to transitions observed in the resonance Raman spectra. The normal mode underlying the transition around 1240 cm^{-1} was identified and found to uniquely refer to the *cis* nature of the 15,15' carbon–carbon double bond.¹⁷

Detailed comparison of resonance Raman spectra and results of DFT calculations also revealed that besides the 15,15'-*cis* configuration another configuration of spheroidene occurs in significant proportion in the reconstituted R26 RC.¹⁷ The DFT calculations for many structures of spheroidene consistently show that two transitions have appreciable intensity in the region

Special Issue: David W. Pratt Festschrift

Received: December 31, 2010

Revised: May 12, 2011

Published: May 23, 2011

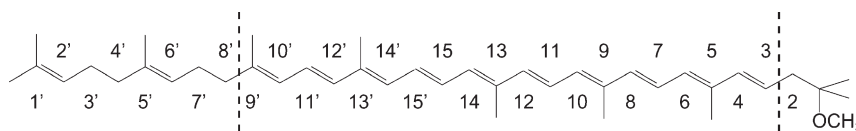


Figure 1. Schematic representation of spheroidene and the labeling of the carbon atoms. The molecule is shown in the all-*trans* form. The dashed lines indicate the conjugated region.

between 1500 and 1570 cm^{-1} of the resonance Raman spectrum, where C=C stretch vibrations typically occur. However, the experimental spectra of several isotopically labeled spheroidenes that were reconstituted into the R26 RC clearly display three or four transitions in this region. This observation can be understood if a second configuration is present. The trend in the shift of the third and fourth transition with the position of the isotope in spheroidene identified the 13,14-*cis* configuration as a likely candidate.

The question remained whether the wild-type RC of *Rb. sphaeroides* contains a second configuration as well, besides the 15,15'-*cis*. The answer to this question is relevant, because the structure and thereby the energy of the triplet state determine the rate of excitation transfer by which spheroidene fulfills its photoprotective function.^{2–4} In addition, it is important to know whether conclusions drawn from studies on the reconstituted R26 RC of *Rb. sphaeroides* apply to the wild type as well, as is suggested by several observations. The structures determined by X-ray diffraction of the reconstituted R26 RC and of the wild-type RC show very similar binding of the carotenoid.^{4,12,13} Also, the electron paramagnetic resonance spectra of the triplet excited spheroidene in wild-type and reconstituted in R26 RC are indistinguishable.¹⁸ However, the resonance Raman spectra recorded with excitation wavelength 496.5 nm of the wild-type RC and the reconstituted R26 RC show minor differences.¹⁹

We compare the resonance Raman spectra acquired at two excitation wavelengths, 496.5 and 514.5 nm, of the wild-type RC and the reconstituted R26 RC. We find that, while spheroidene is present in the reconstituted R26 RC in the 15,15'-*cis* configuration and in another configuration, the wild-type RC contains only 15,15'-*cis* spheroidene. In the resonance Raman spectra of the reconstituted R26 reaction centers a transition is identified that arises exclusively from the second configuration. Mode composition analysis shows that this transition corresponds to a mode that is specific for the 13,14-*cis* configuration.

METHODS

The wild-type RCs were obtained from *Rb. sphaeroides* strain 2.4.1, as described in Shochat et al.²⁰ RCs from *Rb. sphaeroides* R26 were obtained as described in Feher and Okamura.²¹ To reconstitute spheroidene into the R26 RCs, the following procedure was followed. A spheroidene solution in hexane was dispersed in a 1% Triton X-100 solution. To evaporate the hexane, this solution was heated to about 80 °C and stirred until it became clear. The solution was then cooled to room temperature. Solutions of spheroidene prepared in this way remained transparent for several hours at room temperature. Reconstitution was performed by adding the Triton/spheroidene solution to the R26 RCs in TL buffer (10 mM Tris pH 8, 0.1% LDAO, 1 mM EDTA) such that the Triton solution was <0.1% and the spheroidene-RC ratio was 10 and stirring for 6 h. The excess spheroidene was removed by washing the RCs on a DEAE column.

To obtain a glass-like sample at cryogenic temperatures, the samples consisted of one part reaction centers in TL buffer and one part glycerol. This mixture had an optical density of about 0.5 at 496.5 nm. For the resonance Raman experiments a sample volume of 150 μL in a glass tube of 3 mm diameter was used.

Resonance Raman scattering was induced by the 496.5 and 514.5 nm lines of a Spectra Physics model Stabilite 2017 Ar⁺ laser. The scattered light was collected at an angle of 90° and imaged on the entrance slit of an Acton Research SpectraPro-500i spectrograph, which contained a grating of 1200 g mm^{-1} . A notch filter (496.5 nm: Omega Optical Inc., 514.5 nm: Iridian Spectral Technologies) was used to remove light of the excitation wavelength and eliminate “ghost” lines which result from irregularities in the grating. Spectra are collected using a CCD camera (Princeton Instruments Spec-10 system). The dispersion was approximately 1 cm^{-1} per pixel. Calibration was performed using a set of calibration lamps.

Spectra were recorded at a temperature of 77 K. Illumination power was about 100 mW for the spectra recorded at 496.5 nm and about 25 mW for the spectra recorded at 514.5 nm. The illumination time was 10 min.

The vibrational modes of 15,15'-*cis* and 13,14-*cis* and their resonance Raman activity were calculated as described in refs¹⁶ and¹⁷. In short, the Gaussian 03 package, Revision E.01, was used for geometry optimization and subsequent calculation of the Hessian.²² The DFT calculations were performed with the B3LYP functional, and the densities were expressed in a 6-31G* basis. The normal modes and corresponding frequencies were calculated using the Wilson GF formalism using the expressions for the transformation between Cartesian and internal coordinates given by Califano.²³ The internal coordinates were used to estimate the resonance Raman intensities according to

$$I_{\alpha} \propto \nu_{\alpha} \left(\sum_i A_{\alpha i} \delta_i \right)^2 \quad (1)$$

In this formula, ν_{α} is the frequency of the normal mode α , A represents the coordinate transformation matrix and δ_i is the change in internal coordinate i as a result of the (near)-resonant electronic $\pi^* \leftarrow \pi$ transition.²⁴ The strength of the method has been shown by the complete description of the resonance Raman spectra of isotopically labeled all-*trans* spheroidenes in solution.¹⁶

RESULTS AND DISCUSSION

Figure 2 shows the resonance Raman spectra of reconstituted R26 and wild-type RCs recorded at an excitation wavelength of 496.5 nm. In both spectra the resonance Raman transition that is characteristic of the 15,15'-*cis* configuration is observed at 1239 cm^{-1} .¹⁷ To compare the R26 spectra and the wild-type spectra, the spectra were normalized to the integrated intensity of the 1239 cm^{-1} transition, which was determined by fitting a Gaussian function to the transition and taking its surface area. Normalization to this band assures that in both spectra the contribution from the 15,15'-*cis* configuration is the same.

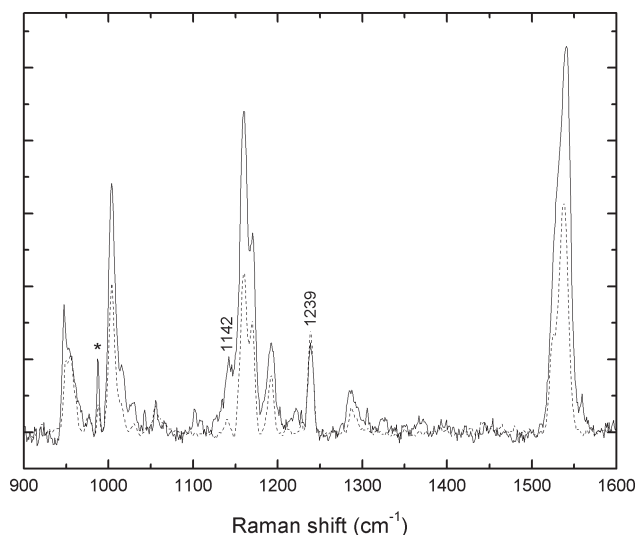


Figure 2. Resonance Raman spectra of reconstituted R26 and wild-type RCs with excitation at 496.5 nm: solid line, R26; dashed line, wild type. The spectra are normalized to the intensity of the 1239 cm^{-1} transition, which is characteristic for the 15,15'-*cis* configuration. The peak denoted with an asterisk is an argon plasma line. A fluorescence background was subtracted.

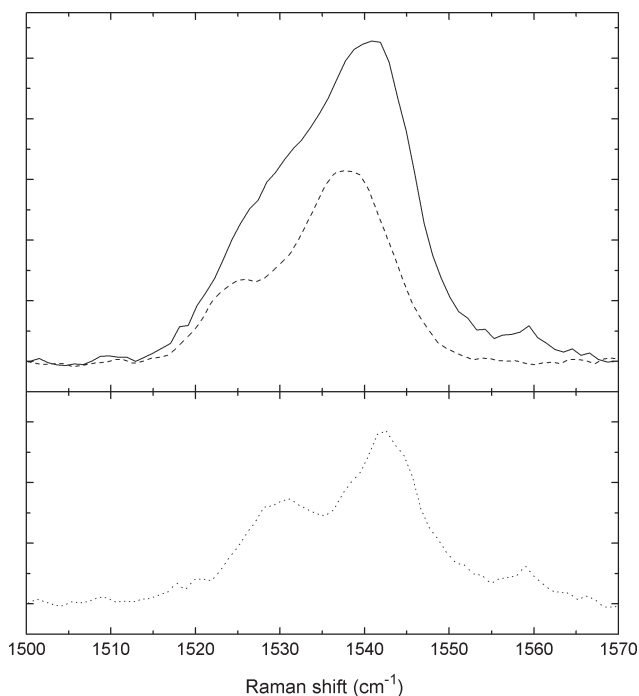


Figure 3. Upper panel: Detail of the resonance Raman spectra of reconstituted R26 (solid line) and wild-type (dashed line) reaction centers. Excitation wavelength: 496.5 nm. The two spectra are normalized to the integrated intensity of the 1239 cm^{-1} transition. Lower panel: Difference of the two spectra shown in the upper panel (R26 – wild type).

Several differences between the reconstituted R26 and the wild-type spectra are observed: (i) the shape of the broad band around 1535 cm^{-1} differs; (ii) upon normalization to the 1239 cm^{-1} transition, the intensity of all other bands is less in the wild-type spectrum than in the R26 spectrum; (iii) the ratio

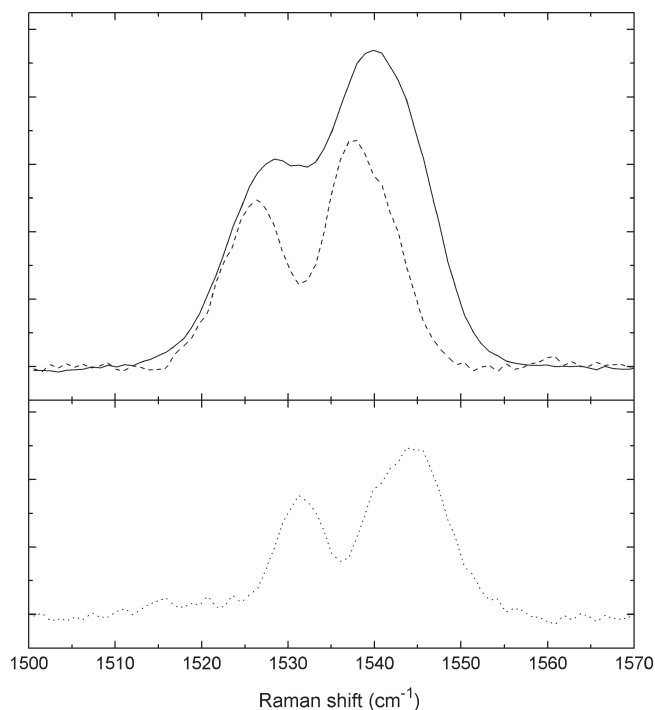


Figure 4. Upper panel: Detail of the resonance Raman spectra of reconstituted R26 (solid line) and wild-type (dashed line) reaction centers. Excitation wavelength: 514.5 nm. The two spectra are normalized to the integrated intensity of the 1239 cm^{-1} transition. Lower panel: Difference of the two spectra shown in the upper panel (R26 – wild type).

of the intensities of the bands at 1158 and at 1170 cm^{-1} is slightly different; and (iv) the wild-type spectrum shows a weak band at 1139 cm^{-1} , while the reconstituted R26 spectrum shows a band at 1142 cm^{-1} of a five times higher intensity. The last three of these differences were already reported by Agalidis et al.¹⁹ but not yet explained.

The upper panel of Figure 3 shows the broad band around 1535 cm^{-1} observed upon excitation at 496.5 nm for both wild type and reconstituted R26 RCs in detail. At cryogenic temperatures, a single resonance Raman transition typically has a width (fwhm) of about 8 cm^{-1} . The band observed at 1535 cm^{-1} for the reconstituted R26 RC appears to arise from more than two transitions. In contrast, the band in the wild-type spectrum may well derive from two transitions.

Resonance Raman spectra of both reconstituted R26 RCs and wild-type RCs were also recorded at the excitation wavelength 514.5 nm (see Supporting Information). The differences between wild-type and reconstituted R26 that were observed at 496.5 nm are also observed in these spectra. The upper panel of Figure 4 shows the broad band around 1535 cm^{-1} at excitation wavelength 514.5 nm in detail. In the wild-type spectrum two transitions are resolved, while the band observed for the reconstituted R26 RCs is again considerably broader.

According to DFT calculations, the resonance Raman spectra of spheroidene will contain two resonance-enhanced Raman transitions in the C=C stretch region between 1500 and 1570 cm^{-1} , independent of the configuration of the carbon chain.^{16,17} The observation of two transitions in this region in the wild-type spectra means that the wild-type RC contains spheroidene in one configuration. The presence of the transition at 1239 cm^{-1} assures that this is the 15,15'-*cis* configuration.

Table 1. Peak Center Positions and Line Widths of the Bands in the 1500–1570 cm^{-1} Region^a

	peak center 1 (cm^{-1})	line width 1 (cm^{-1})	peak center 2 (cm^{-1})	line width 2 (cm^{-1})
WT 514.5	1525.8	8.1	1538.4	9.6
WT 496.5	1524.9	9.3	1537.8	9.3
(R26 – WT) 514.5	1531.2	6.6	1543.9	10.4
(R26 – WT) 496.5	1529.2	10.9	1542.5	11.7

^aThe spectra of wild-type RCs and the spectra resulting from subtraction of the spectrum of the wild-type RC from the spectrum of the reconstituted R26 RC as shown in 3 and 4 were fitted with two Gaussian functions. The error in the distance between two peak center positions within one spectrum as determined by Gaussian fitting is estimated to be at most 2 cm^{-1} .

The lower panels of Figures 3 and 4 display spectra that result from subtraction of the wild-type spectra from the R26 spectra after normalization to the 1239 cm^{-1} transition. These difference spectra also show two transitions, again better resolved for excitation at 514.5 nm.

It is possible to fit two Gaussian functions to the two wild-type spectra and to the two difference spectra. The results of these fits are summarized in Table 1. The centers of the two transitions observed in the wild-type spectra are the same, within the experimental error, at both excitation wavelengths. The same holds for the difference spectra.

From the analysis of the resonance Raman spectra of specific isotope-labeled spheroidenes reconstituted into the R26 RC, Wirtz et al.¹⁷ concluded that besides the 15,15'-*cis* configuration a second configuration of spheroidene is present in the R26 RC. This is confirmed by the presence of two C=C modes in the difference spectra.

The presence of an additional configuration of spheroidene in the R26 RC offers an explanation for the differences between the resonance Raman spectra of wild-type and reconstituted R26 RCs (see Figure 2 and Supporting Information). First, the different shape of the broad band around 1535 cm^{-1} results from the fact that this band derives from two C=C stretch modes for the wild-type RC and from four for the reconstituted R26 RC. Second, the additional configuration is responsible for the “extra” intensity in the R26 spectra as compared to the wild-type spectra after normalization at 1239 cm^{-1} . Third, the shape of the spectrum in the fingerprint region around 1160 cm^{-1} is expected to be different for the two configurations, which explains the difference between the wild-type and reconstituted R26 spectra in this region. Finally, the absence of the transition at 1142 cm^{-1} in the wild-type spectra suggests that this transition corresponds to a mode that is characteristic for the second configuration in the R26 RC.

Wirtz et al.¹⁷ concluded that the isotope-induced shifts of the transitions in the C=C stretch region of the R26 spectra that do not belong to the 15,15'-*cis* configuration, were qualitatively consistent with a 13,14-*cis* configuration. Koyama et al.^{7,8} report on a transition that is typically observed in the 1120–1140 cm^{-1} region of the resonance Raman spectra of isomers of β -carotene that have a 13,14-*cis* bond. We calculated the compositions of the normal modes of spheroidene in the 13,14-*cis* configuration assuming a structure in which the C-atoms of the methyl groups of spheroidene were at the coordinates found from X-ray diffraction by McAuley et al.¹² A mode at 1128 cm^{-1} that is

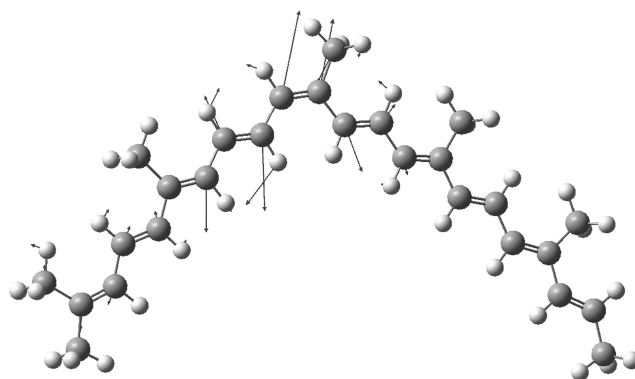


Figure 5. Composition of the normal mode characteristic of the 13,14-*cis* configuration of spheroidene. It is observed in the resonance Raman spectrum of spheroidene in the RC of *Rb. sphaeroides* at 1142 cm^{-1} . The mode consists mainly of single carbon–carbon bond stretches in the region close to the *cis* bond. Arrows indicate relative displacement but are not drawn to scale. Displacement for hydrogen atoms has been scaled down.

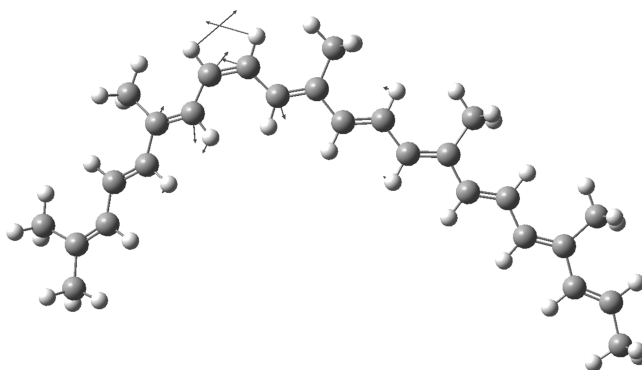


Figure 6. Composition of the normal mode characteristic of the 15,15'-*cis* configuration of spheroidene. It is observed in the resonance Raman spectrum of spheroidene in the RC of *Rb. sphaeroides* at 1239 cm^{-1} . The mode consists almost exclusively of the carbon 14'–15' and 15–14 stretches and the C–H bend vibrations at the 15 and 15' positions. Arrows indicate relative displacement, but are not drawn to scale. Displacement for hydrogen atoms has been scaled down.

characteristic for the 13,14-*cis* configuration and comparable in composition to the 1239 cm^{-1} mode of the 15,15'-*cis* configuration is calculated to gain intensity in a resonance Raman experiment. Both modes consist mainly of two in-phase stretch vibrations of the two single carbon–carbon bonds adjacent to the *cis* bond (see Figures 5 and 6). In the case of the 13,14-*cis* configuration, one of the C-atoms that participates in the *cis* bond has a methyl group attached. Together with a stronger delocalization, this increased mass is responsible for the lower wave-number of this mode for the 13,14-*cis* configuration (1142 compared to 1239 cm^{-1}).

Depending on the preparation of the reconstituted R26 RCs, the ratio of the intensities of the 1158 and 1170 cm^{-1} bands and the shape of the broad band around 1535 cm^{-1} are found to vary (see Supporting Information). The first of these variations was also described in ref 19. The resonance Raman spectra invariably show the presence of both 15,15'-*cis* and 13,14-*cis* spheroidene, as is clear from the presence of the 1239 and the 1142 cm^{-1}

bands. The variations in the spectra can not be fully explained by a change in the relative contributions of the 15,15'-*cis* and the 13,14-*cis* configuration. Instead, they point to a slight variation in the structure of the carotenoid in the RC.

Transient absorption and EPR experiments performed on reconstituted R26 RCs give qualitatively identical results to wild-type RCs.^{18,25,26} A quantitative comparison of the yields of triplet formation is yet to be performed. This could give information on how critical the 15,15'-*cis* configuration of spheroidene is and thereby on the triplet quenching mechanism.

CONCLUSION

Wild-type reaction centers of *Rb. sphaeroides* contain spheroidene in one configuration, namely, 15,15'-*cis*. Reconstituted R26 reaction centers of *Rb. sphaeroides*, on the other hand, contain spheroidene in the 15,15'-*cis* and the 13,14-*cis* configuration. Hence, one must be careful in extrapolating results obtained for the reconstituted R26 reaction center to the wild-type reaction center.

ASSOCIATED CONTENT

S Supporting Information. Resonance Raman spectra of reconstituted R26 and wild-type *Rb. sphaeroides* RCs recorded at excitation wavelength 514.5 nm and a comparison of the resonance Raman spectra of reconstituted R26 RCs for which different reconstitution procedures were followed. This material is available free of charge via the Internet at <http://pubs.acs.org>.

AUTHOR INFORMATION

Corresponding Author

*E-mail: mathies@physics.leidenuniv.nl; groenen@physics.leidenuniv.nl.

ACKNOWLEDGMENT

We acknowledge Florentien Kan for her contribution in the early stages of this project. The research was supported with financial aid by The Netherlands Organization for Scientific Research (NWO), Department of Chemical Sciences (CW).

Work in the laboratory of HAF was supported by a grant from the National Science Foundation (MCB-0913022) and the University of Connecticut Research Foundation.

REFERENCES

- (1) Feher, G.; Allen, J.; Okamura, M.; Rees, D. *Nature* **1989**, *339*, 111–116.
- (2) Cogdell, R. J.; Frank, H. A. *Biochim. Biophys. Acta* **1988**, *895*, 63.
- (3) Frank, H. A.; Cogdell, R. J. *Photochem. Photobiol.* **1996**, *63*, 257–264.
- (4) Hashimoto, H.; Fujii, R.; Yanagi, K.; Kusumoto, T.; Gardiner, A. T.; Cogdell, R. J.; Roszak, A. W.; Isaacs, N. W.; Pendon, Z.; Niedzwiedzki, D.; Frank, H. A. *Pure Appl. Chem.* **2006**, *78*, 1505–1518.
- (5) Lutz, M.; Kleo, J.; Reiss-Husson, F. *Biochem. Biophys. Res. Commun.* **1976**, *69*, 711–717.
- (6) Lutz, M.; Agalidis, I.; Hervo, G.; Cogdell, R. J.; Reiss-Husson, F. *Biochim. Biophys. Acta* **1978**, *503*, 287–303.
- (7) Koyama, Y.; Kito, M.; Takii, T.; Tsukida, K.; Yamashita, J. *Biochim. Biophys. Acta* **1982**, *680*, 109–118.
- (8) Koyama, Y.; Takii, T.; Saiki, K.; Tsukida, K. *Photobiophys.* **1983**, *5*, 139–150.

- (9) Yeates, T. O.; Komiya, H.; Chirino, A.; Rees, D. C.; Allen, J. P.; Feher, G. *Proc. Natl. Acad. Sci. U.S.A.* **1988**, *85*, 7993–7997.
- (10) Arnoux, B.; Ducruic, A.; Reiss-Husson, F.; Lutz, M.; Norris, J.; Schiffer, M.; Chang, C.-H. *FEBS Lett.* **1989**, *258*, 47–50.
- (11) Ermler, U.; Fritzsche, G.; Buchanan, S. K.; Michel, H. *Structure* **1994**, *2*, 925–936.
- (12) McAuley, K.; Fyfe, P. K.; Ridge, J. P.; Cogdell, R. J.; Isaacs, N. W.; Jones, M. R. *Biochemistry* **2000**, *39*, 15032–15043.
- (13) Roszak, A. W.; McKendrick, K.; Gardiner, A. T.; Mitchell, I. A.; Isaacs, N. W.; Cogdell, R. J.; Hashimoto, H.; Frank, H. A. *Structure* **2004**, *12*, 765–773.
- (14) Kok, P.; Köhler, J.; Groenen, E. J.; Gebhard, R.; van der Hoef, I.; Lugtenburg, J.; Hoff, A. J.; Farhoosh, R.; Frank, H. A. *Biochim. Biophys. Acta* **1994**, *1185*, 188–192.
- (15) Kok, P.; Köhler, J.; Groenen, E. J.; Gebhard, R.; van der Hoef, I.; Lugtenburg, J.; Farhoosh, R.; Frank, H. A. *Spectrochim. Acta, Part A* **1997**, *53*, 381–392.
- (16) Dokter, A. M.; van Hemert, M. C.; in 't Velt, C. M.; van der Hoef, K.; Lugtenburg, J.; Frank, H. A.; Groenen, E. J. *J. Phys. Chem. A* **2002**, *106*, 9463–9469.
- (17) Wirtz, A. C.; van Hemert, M. C.; Lugtenburg, J.; Frank, H.; Groenen, E. J. *Biophys. J.* **2007**, *93*, 981–991.
- (18) Chadwick, B. W.; Frank, H. A. *Biochim. Biophys. Acta* **1986**, *851*, 257–266.
- (19) Agalidis, I.; Lutz, M.; Reiss-Husson, F. *Biochim. Biophys. Acta* **1980**, *589*, 264–274.
- (20) Shochat, S.; Arlt, T.; Francke, C.; Gast, P.; van Noort, P. I.; Otte, S. C. M.; Schelvis, H. P. M.; Schmidt, S.; Vijgenboom, E.; Vrieze, J.; Zinth, W.; Hoff, A. J. *Photosynth. Res.* **1994**, *40*, 55–66.
- (21) Feher, G.; Okamura, M. Y. Chemical composition and properties of reaction centers. In *The Photosynthetic Bacteria*; Clayton, R. K., Sistrom, W. R., Eds.; Plenum Press: New York, 1978; Chapter 19, pp 349–386.
- (22) Frisch, M. J. et al. *Gaussian 03*, Revision E.01; Gaussian, Inc.: Wallingford, CT, 2004.
- (23) Califano, S. *Vibrational States*; Wiley: London, 1976.
- (24) Myers, A. B.; Harris, R. A.; Mathies, R. A. *J. Chem. Phys.* **1983**, *79*, 603–613.
- (25) Frank, H. A.; Violette, C. A. *Biochim. Biophys. Acta* **1989**, *976*, 222–232.
- (26) Farhoosh, R.; Chynwat, V.; Gebhard, R.; Lugtenburg, J.; Frank, H. A. *Photochem. Photobiol.* **1997**, *66*, 97–104.
- (27) de Groot, H. J.; Gebhard, R.; van der Hoef, I.; Hoff, A. J.; Lugtenburg, J.; Violette, C. A.; Frank, H. A. *Biochemistry* **1992**, *31*, 12446–12450.